Efficient high-energy pulse-train generation using a 2^n-pulse Michelson interferometer

Craig W. Siders, Jennifer L. W. Siders, Antoinette J. Taylor, Sang-Gyu Park, and Andrew M. Weiner

We demonstrate a novel, Michelson-based, ultrafast multiplexer with a throughput approaching 100% for a polarization-multiplexed train and 50% for a linearly polarized train, which is compatible with a high-energy pulse train and shaped-pulse generation. The interpulse spacings in the resultant 2^n-pulse train can be adjusted continuously from multinanoseconds through zero. Using this interferometer, we also demonstrate generation of a 16-pulse train of terahertz pulses. © 1998 Optical Society of America

OCIS codes: 120.3180, 120.4820, 140.7090, 320.5540, 320.7160, 060.4230.

1. Introduction

Numerous applications currently exist that require a train of high-energy ultrafast pulses. Such applications include multiple-laser-pulse excitation schemes for high-gradient plasma accelerators,[1] photocathode injectors for conventional accelerators, multiple-pulse excitation of atoms, molecules, and solids,[2] and high-fluence terahertz wave-train generation for radar and microwave communications.[3] Moreover optimization of the efficiency of high-harmonic generation when short pulses are used may require the use of fast-rise-time flat-top pulses. Such super-Gaussian pulses can be generated when several short pulses are stacked together with an interpulse spacing of the order of the initial short-pulse width.[4]

Pulse-shaping techniques in which phase and amplitude masks are used in the focal plane of a zero-dispersion pulse stretcher are typically used for producing low-energy (i.e., oscillator-level) ultrafast shaped pulses and pulse trains.[5] Using such techniques to produce trains of high-energy (i.e., amplified) pulses is limited because of damage to the mask residing in the focal plane of the stretcher. Pulse shaping of 200-μJ pulses by using an acousto-optic modulator has recently been demonstrated;[6] however, the setup exhibits 2 orders of magnitude loss, resulting in only a 2-μJ output. A further increase in the diffraction efficiency causes significant acoustic nonlinearity in the acousto-optic modulator. Pulse shaping before amplification has been demonstrated,[7] but care must be taken to avoid nonlinear effects, such as nonlinear temporal diffraction,[8] that occur with amplitude masking. Even in the case of phase-only masking, amplifier output fluences are typically reduced compared with that from an unshaped input. Finally, the experimental necessity of a single short pulse synchronized to the pulse train for cross-correlation measurements ultimately dictates that pulse shaping occur after amplification.

Several schemes have appeared in the literature that are variations on a Michelson interferometer using multiple beam splitters and optical delay lines to produce pulse trains of 2^n pulses where n is a positive integer.[9,10] These schemes do not propagate the beam through a focus and therefore are compatible with pulse shaping high-energy pulses. The n-fold application of a single Michelson interferometer would appear at first glance to reduce the total fluence of the generated train to 2^{-n} because each unit has a single beam on the input and two beams on the output, one of which is not used. Similar conclusions on generation efficiency are reached for pulse-train generation when a series of beam splitters is used.[10] When both beams from each beam splitter were used, the generation of two output beams that contain sequences of 2^n pulses has been demonstrated.[9] However, interpulse spacings in this device are limited by optical elements to >100 ps,

C. W. Siders, J. L. W. Siders, and A. J. Taylor are with the Materials Science and Technology Division, Los Alamos National Laboratory, MS D429, Los Alamos, New Mexico 87545. S.-G. Park and A. M. Weiner are with the School of Electrical and Computer Engineering, Purdue University, West Lafayette, Indiana 47907.

Received 15 December 1997; revised manuscript received 26 March 1998.

0003-6935/98/225302-04$15.00/0

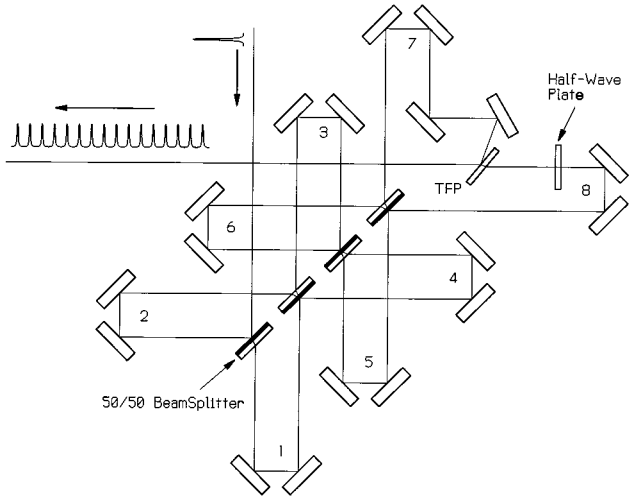

Fig. 1. Interferometer design for generation of a train of 16 pulses. For equally spaced pulses, arm 2 is lengthened by half a unit, arm 3 by one unit, arm 6 by two units, and arm 8 by four units.

and therefore it is unsuitable for ultrashort-pulse multiplexing.

2. *n*-Fold Michelson Interferometer

We present here an n-fold application of a Michelson interferometer, which, by using both beams from each beam splitter and then by polarization multiplexing the two output beams, results in a single pulse train of 2^n pulses with nearly 100% throughput. In the frequency domain this interferometer represents, for each polarization, a highly oscillatory amplitude and phase filter. Our device design for the generation of a train of 16 pulses is shown in Fig. 1. Because the delay arms can be easily positioned for equal lengths, interpulse spacings from zero to multinanoseconds are achievable. The first eight pulses are orthogonally polarized to the final eight; however, one can easily polarize the output along a single axis by using a high-damage-threshold thin-film polarizer, resulting in a 50% throughput. In some cases, for example, a laser-driven e^+/e^- collider, the two linearly polarized output trains can be individually used. In general, for a 2^n pulse train the design shown in Fig. 1. requires n beam splitters, $(4n + 2)$ mirrors, $2n$ linear translators (to set and vary the interpulse spacing), one half-wave plate, and one thin-film polarizer, leading to a cost that scales as n and an overall area that scales as n^2.

To characterize this device, we use the 800-nm, 150-fs, 1-mJ output of a chirped-pulse amplified Ti: sapphire laser system operating at 1 kHz. For a 16-pulse interferometer 18 mirrors and 4 beam splitters are needed. For reduced cost, protected gold-coated mirrors and dielectric beam splitters are used, resulting in a measured throughput of 73%, as expected. If we were to use high-damage-threshold dielectric mirrors, a throughput of 98% would be expected. The interferometer is initially aligned so that the pulses overlap temporally two at a time. Such temporal overlap is determined first with spatial fringes and is optimized with second-harmonic generation in a doubling crystal. The desired pulse sequence is then set. For equally spaced pulses out of the interferometer in Fig. 1, arm 2 is lengthened by half a unit, arm 3 by one unit, arm 6 by two units, and arm 8 by four units. For the data shown in Fig. 2 the interferometer is configured with 3-ps pulse separations and the output is cross-correlated with a single gate pulse, split off before the interferometer, in a 0.5-mm-thick KDP crystal. When individual arms are blocked in the interferometer, various pulse sequences can be formed as shown in Fig. 2, including the elimination of every other pulse in the pulse train as well as double-pulse and quadruple-pulse bursts.

Complete pulse-train characterization can be achieved by blocking appropriate arms within the interferometer to allow the passage of each of the 16 pulses individually, allowing the linear measurement of individual energies as well as the nonlinear cross-correlation profiles of each pulse. Note that the en-

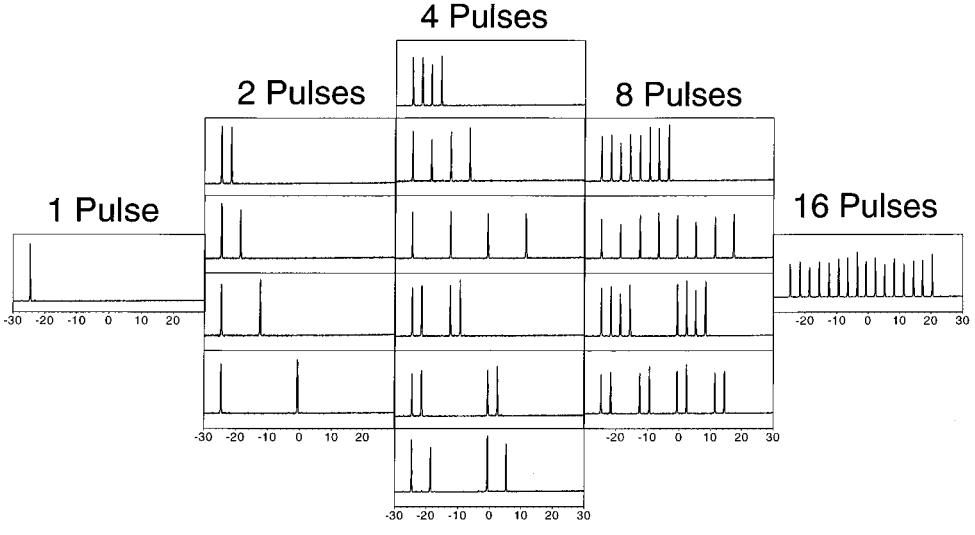

Fig. 2. With the 16-pulse interferometer configured for 3-ps pulse separations, blocking particular arms produces these and similar pulse trains. For these data the output of the interferometer is cross-correlated with a single gate pulse, split off before the interferometer, in a 0.5-mm KDP crystal.

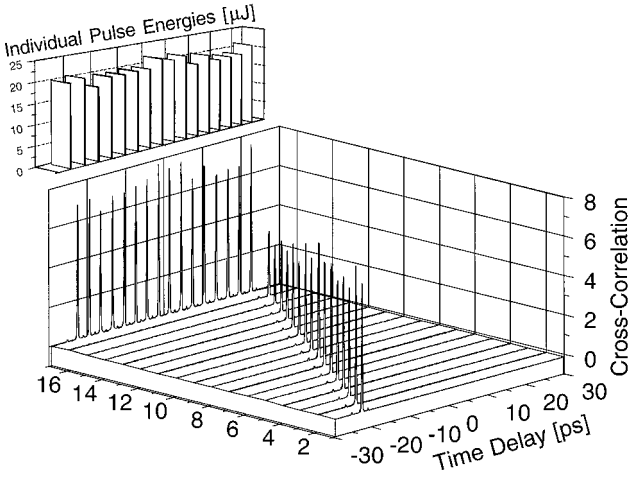

Fig. 3. Linear power meter (Molectron PM3) measurements of the pulse energies (top) and cross correlation of each pulse separately as well as a cross correlation of the full pulse train (bottom). Note the good agreement between the linear measurements of pulse energy and the full-train cross-correlation.

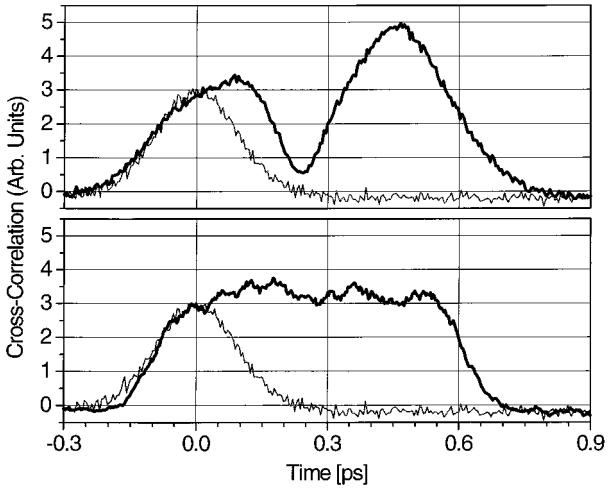

Fig. 4. (Top) Output of the interferometer configured to produce a dark pulse. To produce this output, four pulses separated by 200 fs were stacked together with the second pair of pulses out of phase from the first pair by π. (Bottom) Output of the interferometer configured to produce a super-Gaussian pulse. To produce this output, four pulses separated by 200 fs were stacked together in phase.

ergy of each pulse in the train is constant for all output sequences. Figure 3 demonstrates such a characterization of the device with linear power meter (Molectron PM3) measurements of the pulse energies (top) and nonlinear cross correlation of each pulse separately as well as a cross correlation of the full 16-pulse train (bottom). The small subpulses present in the cross-correlation measurements result from a reflection off a beam splitter placed before the interferometer. We measure a variation of $<20\%$ in both pulse output energy and intensity over the entire 16-pulse train.

3. Pulse Stacking: Dark-Pulse and Super-Gaussian Pulse Generation

This interferometer can also be used to stack several short pulses together with an interpulse spacing comparable with or less than the input pulse width. In this case the output pulse structure depends on the relative phase shift between the overlapping multiplexed pulses. Since the phase difference between the reflected and the transmitted pulses from a dielectric beam splitter is approximately π, a dark pulse, in which a nearly constant high-intensity field rapidly goes to zero and returns on an ultrafast time scale, can be produced by stacking a series of pulses of one phase next to a series of pulses with the opposite phase, as shown in Fig. 4 (top). Moreover stacking several pulses together in-phase with pulse separations comparable with their pulse widths results in a super-Gaussian pulse [shown in Fig. 4 (bottom)], potentially useful for efficient high-harmonic generation.

4. Terahertz Wave-Train Generation in DAST

As a final application of this technology, we generated a 16-pulse train of terahertz pulses through optical rectification in dimethyl amino 4-N-methylstilbazolium tosylate (DAST). DAST is an electro-optic material and an efficient unbiased terahertz emitter, exhibiting saturation in its terahertz output[11] only for optical fluences of >20 mJ/cm^2. For total excitation fluences below this value, the terahertz output is expected to depend linearly on the optical pulse train generated by the interferometer. Coherent detection of the terahertz wave form by using a radiation-damaged silicon-on-sapphire photoconductive detector with a 2-mm-wide gap, gated by a single optical pulse split off from the pulse train before the interferometer, results in a temporal resolution of 1 ps. Figure 5 reveals the terahertz pulse trains resulting from multipulse (1, 2, 4, 8, and 16) excitation of DAST with a pulse separation of 3 ps. No sign of saturation is present in the wave forms.

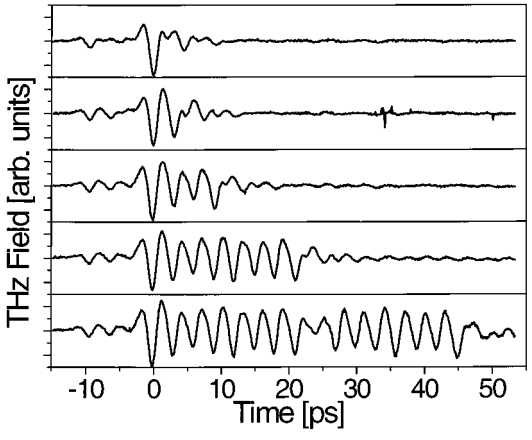

Fig. 5. Terahertz pulse trains resulting from a multipulse (1, 2, 4, 8, and 16) optical excitation of DAST with a pulse separation of 3 ps. The optical pulse trains were generated with the interferometer shown in Fig. 1.

Terahertz pulse-train generation (of as many as five pulses), also in DAST, has been demonstrated previously[12] by using zone plates consisting of thin glass slides to generate the low-fluence optical excitation train. Although this approach is perhaps simpler than our approach, it lacks the flexibility to change the interpulse separation, to utilize high optical fluences, to pick out a specific pulse sequence, and to characterize each pulse separately. Moreover, since detection of the generated pulses was performed with a Michelson interferometer, the spectrum and not the temporal wave form of the generated terahertz pulse was measured. We expect such terahertz pulse trains to be used as sources for microwave and radar communications, as tunable, coherent radiation sources in the far IR, and as sources of terahertz pulse trains for coherent control experiments.[13]

5. Summary

In summary, we have demonstrated a novel ultrafast multiplexer with a throughput approaching 100% for a polarization-multiplexed train and 50% for a linearly polarized train, which is compatible with high-energy pulse-train and shaped-pulse generation. The interpulse spacings in the resultant 2^n-pulse train can be adjusted continuously from multinanoseconds through zero. Consisting entirely of passive optical elements and simple linear delay stages, this multiplexer can be implemented in miniature with existing nanotechnology[14] for low power, high-pulse-count applications. For example, an 8-bit, 256-pulse interferometer, although cumbersome to build with optics 1-in. (2.5 4-cm) in diameter, could be fabricated with less than a 1-cm^2 footprint.

References

1. D. Umstadter, E. Esarey, and J. Kim, "Nonlinear plasma waves resonantly driven by optimized laser pulse trains," Phys. Rev. Lett. **72,** 1224–1227 (1994).
2. R. J. Temkin, "Excitation of an atom by a train of short pulses," J. Opt. Soc. Am. B **10,** 830–839 (1993).
3. Y. Liu, S.-G. Park, and A. M. Weiner, "Enhancement of narrow-band terahertz radiation from photoconducting antennas by optical pulse shaping," Opt. Lett. **21,** 1762–1764 (1996).
4. I. P. Christov, M. M. Murnane, and H. C. Kapteyn, "High-harmonic generation of attosecond pulses in the 'single-cycle' regime," Phys. Rev. Lett. **78,** 1251–1254 (1997).
5. A. M. Weiner, J. P. Heritage, and E. M. Kirshner, "High-resolution femtosecond pulse shaping," J. Opt. Soc. Am B **5,** 1563–1572 (1988).
6. C. J. Bardeen, V. V. Yakovlev, K. R. Wilson, S. C. Carpenter, P. M. Weber, and W. S. Warren, "Feedback quantum control of molecular electronic population transfer," Chem. Phys. Lett. **280,** 151–158 (1997).
7. M. Dugan, J. X. Tull, J.-K. Ree, and W. S. Warren, "High-resolution ultrafast laser pulse shaping for quantum control and terabit per second communications," in *Ultrafast Phenomena X*, P. F. Barbara, J. G. Fujimoto, W. H. Knox, and W. Zinth, eds. (Springer-Verlag, Berlin, 1996), pp. 26–27.
8. X. Liu, R. Wagner, A. Maksimchuk, E. Goodman, J. Workman, D. Umstadter, and A. Migus, "Nonlinear temporal diffraction and frequency shifts resulting from pulse shaping in chirped-pulse amplification systems," Opt. Lett. **20,** 1163–1165 (1995).
9. C. E. Clayton, N. A. Kurnit, and D. D. Meyerhofer, "Application of conventional laser technology to gamma–gamma colliders," Nucl. Instrum. Methods A **355,** 121–129 (1995).
10. W. E. Martin and D. Milam, "Interpulse interference and passive laser pulse shapers," Appl. Opt. **15,** 3054–3061 (1976).
11. T. J. Carrig, G. Rodriguez, T. S. Clement, A. J. Taylor, and K. R. Stewart, "Scaling of terahertz radiation via optical rectification in electro-optic crystals," Appl. Phys. Lett. **66,** 121–123 (1995).
12. C. Messner, M. Sailer, H. Kostner, and R. A. Höpfel, "Coherent generation of tunable, narrow-band THz radiation by optical rectification of femtosecond pulse trains," Appl. Phys. B **64,** 619–621 (1997).
13. P. G. Huggard, J. A. Cluff, C. J. Shaw, S. R. Andrews, E. H. Linfield, and D. A. Ritchie, "Coherent control of cyclotron emission from a semiconductor using subpicosecond electric field transients," Appl. Phys. Lett. **71,** 2647–2649 (1997).
14. M. C. Wu, L.-Y. Lin, S.-S. Lee, and K. S. J. Pister, "Micromachined free-space integrated micro-optics," Sensors Actuators **50,** 127–134 (1995).